scientific reports

Check for updates

OPEN

Characterization of a chemically induced osteoarthritis model in zebrafish

Gongyi Xiao[1,4,6], Jin Qin[2,6], Huiping Yang[3], Qizhi Song[4], Ruobin Zhang[5], Junlan Huang[5], Yuexi Mou[1], Wen Liu[1], Xianding Sun[1]✉ & Mao Nie[1]✉

Osteoarthritis (OA) is characterized by the progressive degeneration of the synovial joint, leading to irreversible damage to articular cartilage and subchondral bone. While animal models have advanced our understanding of OA, numerous unresolved issues still remain. The zebrafish, known for its transparent body, rapid developmental, and impressive regenerative capabilities, offers substantial potential for osteoarthritis research. This study seeks to establish a new OA model utilizing the zebrafish jaw joint, acting as a supplement to traditional animal models. In the future, this model could serve as a valuable platform for delving deeper into the mechanisms of this disease, as well as for advancing drug discovery and therapeutic interventions. Leveraging the skeletal structure of zebrafish, we targeted the largest jaw joint for our research. A custom fixation device was crafted, and a microinjection system was utilized to inject mono-iodoacetate (MIA) or collagenase type II (CTII) into the joint cavity of zebrafish. Subsequent analyses included histological staining, immunohistochemistry, OA research society international (OARSI) scoring, and real-time in vivo imaging were performed at 7, 14, and 28 days post injection. Our results effectively demonstrated the presence of synovial inflammation and cartilage damage within the zebrafish mandible, affirming the feasibility of inducing OA in zebrafish. In conclusion, the local injection of chemical agents into the joint cavity of zebrafish effectively induced the occurrence of OA. Establishing the zebrafish OA model enhances the array of animal models available for OA research. Moreover, zebrafish present distinct advantages, including robust regenerative abilities, genetic editing simplicity, and efficient drug screening. Consequently, this offers a fresh avenue for investigating the pathogenesis, prevention, and potential therapeutic approaches for human OA.

Keywords Osteoarthritis, Zebrafish model, Jaw joint, Mono-iodoacetate, Collagenase type II

Abbreviations

OA	osteoarthritis
MIA	mono-iodoacetate
CTII	collagenase type II
OARSI	OA Research Society International
OMD	osteomodulin
TCC	triclocarban
dpi	days post injection
H&E	hematoxylin & eosin MMP13:matrix metalloproteinase 13
PBS	phosphate-buffered saline
SD	standard deviation
ANOVA	analysis of variance

[1]Center for Joint Surgery, Department of Orthopedic Surgery, The Second Affiliated Hospital of Chongqing Medical University, 74 Linjiang Road, Chongqing 400010, China. [2]Center for Spinal Surgery, Department of Orthopedic Surgery, The Second Affiliated Hospital of Chongqing Medical University, 74 Linjiang Road, Chongqing 400010, China. [3]Department of Cardiology, The Second Affiliated Hospital of Chongqing Medical University, 74 Linjiang Road, Chongqing 400010, China. [4]Department of Orthopedic Surgery, Chonggang General Hospital, No. 1 Dayan Sancun, Dadukou District, Chongqing 400000, China. [5]Department of Wound Repair and Rehabilitation Medicine, State Key Laboratory of Trauma, Burns and Combined Injury, Trauma Center, Research Institute of Surgery, Daping Hospital, Army Medical University, Chongqing 400042, China. [6]Gongyi Xiao and Jin Qin contributed equally to this work. ✉email: xianding@hospital.cqmu.edu.cn; 302218@cqmu.edu.cn

GAG glycosaminoglycan

Osteoarthritis (OA) is a prevalent chronic and painful disease characterized by joint cartilage degradation and joint inflammation[1–3]. This disease results in joint dysfunction, pain and disability, significantly imparing patients' quality of life[4,5]. The pathological progression of OA involves inflammatory responses, cartilage degradation, osteophyte formation, and alterations in subchondral bone[6]. Current researches focus on uncovering the molecular mechanisms driving OA pathogenesis and developing effective treatment strategies, as existing therapies typically address symptoms rather than the root causes of the condition. Establishing stable and reliable animal models is crucial for OA research, providing valuable insights into disease mechanisms and aiding in the evaluation of potential therapeutic strategies. Existing animal models of OA primarily utilize mice[7–9], rats[10,11] and rabbits[12,13], induced through surgery, drug treatment or gene editing[14,15]. These models offer advantages such as maturity, controllability and ease of manipulation[16,17]. However, While they can closely mimic the actual disease state, the complexity of their biological systems often poses challenges for researchers in interpreting outcomes directly. On the other hand, traditional in vitro culture systems lack the ability to capture in vivo interactions fully. Therefore, there is a growing need for a more streamlined system that can effectively facilitate in vivo research.

Zebrafish, as an innovative model organism, presents unique advantages such as transparent embryos, convenient genetic editing, affordability, and rapid growth[18,19]. Previous work by R. E. Mitchell et al.[20] highlighted the utility of zebrafish in OA research. More recently, Jérémie Zappia et al.[21] explored the impact of osteomodulin (OMD) in OA by inducing mutations in zebrafish. Studies have also demonstrated that exposure to Triclocarban (TCC) can induce OA in the anal fin of zebrafish. Additionally, research by Joanna Smeeton et al.[22] showcased the regenerative potential of zebrafish cartilage. Together, these findings emphasize the significant research opportunities and value of zebrafish in OA studies.

In traditional animal models utilizing chemicals to induce OA, researchers commonly use collagenase type II (CTII) or mono-iodoacetate (MIA) injections into the knee joint. Studies on zebrafish have identified the jaw joint as a synovial joint[23,24], proving a unique opportunity for OA research. After carefully evaluating the overall structure of zebrafish and considering experimental design and feasibility, we chosed to induce OA in the zebrafish's jaw joint. Initially, we utilized the transgenic fish line *Tg (col2a1a: EGFP)* cq77, which marks cartilage, to observe the expression pattern in the jaw cartilage. Subsequently, we designed a simple and reliable device using a microinjection system and induced OA phenotypes via single injections of MIA[10] and CTII[25]. Tissue samples were collected at 7, 14 and 28 days post injection (dpi). Various experimental techniques, including histological staining, OA scoring, immunohistochemistry and in vivo fluorescence imaging were employed to examine the pathological and physiological changes of OA in the zebrafish jaw joint.

Our research underscores the potential of utilizing zebrafish to establish novel OA models, offering fresh insights and methodologies for OA research.

Methods

Zebrafish strains and generation of transgenic lines

The AB and transgenic fish lines employed in this study were sourced from the Zebrafish Resource Center of China. All zebrafish were housed in semi-closed recirculation housing systems manufactured by ESEN, China, and were maintained at a constant temperature of 28.5 °C on a 14:10 h light: dark photoperiod. The care and maintenance of all zebrafish lines strictly followed standard protocols[26]. Zebrafish were anesthetized by immersed in 0.2% tricaine (#A5040, Sigma-Aldrich, America) for 30 s. The in vivo experiments and associated protocols were conducted in accordance with ethical guidelines and received approval from the Institutional Animal Care and Use Committee of the Research Institute of Surgery, Daping Hospital, under IACUC protocol SYXK-(Army) 2022-0003. All animal experiments were carried out in strict compliance with the ethical guidelines outlined in the National Institutes of Health guide for the care and use of Laboratory Animals and the ARRIVE (Animal Research: Reporting In Vivo Experiments). These measures were implemented to ensure the ethical treatment and welfare of the zebrafish subjects, as well as to uphold the scientific integrity of the research.

Zebrafish mandibular joint injection device

Crafted as a meticulously designed tool, this device serves the purpose of precisely administering drugs into the zebrafish jaw joint. It was crafted to accommodate the anatomical characteristics of the joint, ensuring easy access while minimizing potential damage to the surrounding tissues during the injection process. The core components of this injection device include a fixture, injection needle, syringe, injection platform, and an external light source. To construct the fixture, 0.3 g of agarose is dissolved in 30 mL of ddH2O, necessitating heat during the dissolution. The solution is then slowly poured into a 10 cm Petri dish, where a 2–3 mm thick barrier is inserted. Once the solution solidifies at room temperature, the barrier is removed. The injection needle is crafted using a single-channel thin-walled glass capillary (#TW100-4, World Precision Instruments, USA). This glass tube is affixed to a horizontal puller (#PN-30, Narishige, Japan) and swiftly heated. As the glass tube softens, it is horizontally drawn to create a needle with a sealed tip. Subsequently, the needle undergoes precision trimmed using a 15° bevel cutting knife under a microscope to establish an aperture. Operation of the syringe involves a pneumatic micro-pump (#PV820, WPI, USA) to regulate injection pressure effectively. The injection platform comprises a stereo microscope (#SZX2-ILLD, Olympus, Japan), complemented by an external light source (#LG-PS2-5, Olympus, Japan) to facilitate the administration process.

Intra-articular injection of mono-iodoacetate or collagenase in the jaw joint

The 45 AB zebrafish individuals (1 year old) were randomly and equally divided into three groups, each containing 15 zebrafish. The control group received intra-articular injections of sterile saline (0.9% NaCl), whereas the experimental groups were administered with 3% mono-iodoacetate dissolved in sterile saline (30 mg/ml) and 1% collagenase type II dissolved in sterile saline (10 mg/ml) respectively. Following the injections, histological assessments will be conducted at 7, 14 and 28 dpi, with 5 zebrafish randomly selected from each group at each time point to assess the effects of drugs on the jaw joint tissues.

Zebrafish whole skeleton staining

The process of performing whole skeleton staining in zebrafish comprises several crucial steps to achieve successful visualization of the skeletal structure. Initially, we humanely euthanized the selected zebrafish using a cold shock method[27]. The zebrafish were placed in ice, maintaining a cold environment for 15–20 min after gill movement ceased. After removing the internal organs, the zebrafish were fixed in a 15 mL centrifuge tube with 95% ethanol for 3 days. Subsequently, the ethanol was removed, and samples were immersed in acetone for 2 days. A fresh staining solution was prepared by mixing 1 mL of 0.3% Alcian Blue in 70% ethanol, 1 mL of 0.1% Alizarin Red in 95% ethanol, 1 mL of glacial acetic acid and 17 mL of 70% ethanol. The acetone was then replaced with the staining solution, allowing it to incubate with the sample for 2–3 days. Afterward, the staining solution was removed, and 1% KOH was introduced to digest the tissue surrounding the skeleton. During the digestion process, the 1% KOH solution was refreshed on the 3rd day for adult fish, and a gradient of 1% KOH/glycerol (75%, 50%, 25%) was used after the 7th day until the tissues surrounding the skeleton were completely digested. The skeletal structures were preserved in glycerol, and images were captured using a fluorescence microscope (Zeiss).

The preparation of paraffin sections from zebrafish

Initially, the zebrafish was humanely euthanized, and its head was delicately positioned in a 15 mL centrifuge tube, where it was fixed overnight at 4 °C in 4% PFA. Following this, the samples underwent a decalcification process by being immersed in 15% EDTA/PBS (pH 7.0) at room temperature for 10–12 days. After decalcification, the tissues were dehydrated through a series of alcohol gradients: 75%, 85%, 90% and 95% ethanol, each for 30 min, followed by two changes of 100% ethanol for 30 min each. Subsequently, the tissues were clarified in xylene for approximately 20 min, then infiltrated with paraffin for 4–6 h before finally embedded. Using a paraffin microtome (Leica), continuous sections with a thickness of 5 μm were meticulously obtained. These sections were air-dried and prepared for subsequent experiments.

Histology staining

To achieve intact paraffin sections of the zebrafish mandibular joint suitable for Safranin O/Fast Green and hematoxylin & eosin (H&E) staining, the following detailed protocols should be meticulously followed:

1. Place paraffin sections in a 60 °C oven and bake for 30 min.
2. De-wax the sections in xylene for 20 min, followed by rehydration through a series of graded alcohols (absolute ethanol, 95% ethanol, 75% ethanol), and a final rinse in distilled water.
3. For Safranin O/Fast Green staining, immerse the sections in 0.1% Safranin solution for 3 min, then quickly rinse in distilled water to prevent fading. Subsequently, immerse the sections in 0.1% Fast Green solution for 3–10 s, adjusting timing baed on desired staining effect. Briefly rinse the Sects. 1–3 times in 1% acetic acid solution, followed by distilled water, 95% ethanol, air-dry and mount with neutral resin.
4. For H&E staining, immerse the sections in hematoxylin for 2 min, followed by a distilled water rinse for 3–5 min. Evaluate the staining intensity under a microscope and adjust if necessary. If needed, decolorize with acid alcohol, rinse, immerse in eosin for 15 s, followed by ethanol rinses. Adjust attaining as needed and finish with a distilled water rinse, air-dry and mount with neutral resin for observation under an inverted fluorescence microscope.

Immunohistochemical analysis

The immunohistochemical analysis was conducted using a two-step tissue staining kit (#PV-9001, ZSGB-BIO, CHINA). Initially, the endogenous peroxidase activity was neutralized using 3% H2O2 (Reagent 1), followed by antigen retrieval with 0.1% trypsin for 10–15 min. Subsequently, the sections were incubated overnight at 4 °C with specific antibodies targeting AGGRECAN (dilution 1:100, #AB1031, Abcam), Adamts5 (dilution 1:100, #DF13268, Chondrex), and matrix metalloproteinase 13 (MMP13) (dilution 1:300, #18165-1AP, Proteintech). Afterward, the sections were rinsed with phosphate-buffered saline (PBS) and incubated with 100 μl reaction enhancer (Reagent 2) at room temperature for 20 min, followed by a tertiary wash with PBS. Subsequent steps included adding an appropriate amount of enhanced polymer enzyme conjugate (Reagent 3), incubating at room temperature for 20 min, another wash, and the addition of freshly prepared DAB chromogenic solution. Following a 1–3 min incubation at room temperature, the sections were counterstained with methyl green. Cell counting was conducted within the cartilage regions of the mandibular joint. The quantification of positively stained cells in the articular cartilage regions was performed using Image 1.54f software. Three sections were selected for assessment per sample, and the average count across these sections was calculated for each sample.

Zebrafish OA research society international(OARSI) scoring and statistical analysis

In all experiments, 1-year-old zebrafish and corresponding age-matched control zebrafish were employed. The OARSI scoring for zebrafish was conducted following the method outlined by Askary et al.[22,23]. For each of the

three joint images, grade and stage values were assigned to both the anterior (anguloarticular) and posterior (quadrate) surfaces. The score for each individual articular surface was computed by multiplying its grade and stage values. Subsequently, the scores of the joint surfaces were averaged for each animal. Two independent researchers evaluated 3–4 representative Safranin O/Fast Green-stained images of the induced joint in each experiment for OARSI scoring in a blinded manner. All numerical data were presented as the mean ± standard deviation (SD), with error bars indicating SD. Statistical analysis entailed comparing differences between two groups using unpaired Student's t-test and analysis of variance (ANOVA) for comparisons involving multiple groups. Post hoc testing using Tukey's method was carried out upon reaching statistical significance levels ($P < 0.05$). The statistical analysis was carried out using GraphPad PRISM 9.0 software, with statistical significance set at $P < 0.05$.

Live imaging

At 14 and 28 dpi, *Tg (col2a1a: EGFP)* cq77 zebrafish were anesthetized using 0.2% tricaine (#A5040, Sigma-Aldrich, America) and then immobilized in 1% low-melting-point agarose within a confocal dish. Fluorescence imaging of the live zebrafish mandibular joints was conducted using a Zeiss confocal microscope. This approach facilitated the non-invasive visualization and evaluation of the dynamic changes occurring in the *Tg (col2a1a: EGFP)* cq77 zebrafish mandibular joints at specific time points following the injury.

Statistical analysis

All numerical data were presented as mean ± SD, with error bars representing SD. Statistical analysis included the utilization of unpaired two-sample Student's t-test to compare differences between two groups and ANOVA for comparisons among multiple groups.

Results

The zebrafish jaw joint was designated as a modeling joint

To investigate the feasibility of establishing an OA model in zebrafish mandibular joint, we initially examined the cartilage within the jaw joint. Leveraging the transgenic zebrafish line *Tg (col2a1a: EGFP)* cq77, recognized for cartilage labeling, we conducted live imaging assessments of the mandibular joints in one-year-old adult zebrafish. These observations revealed notable Col2a1a expression on the surfaces of the anguloarticular bone and quadrate bone within the jaw joint (Fig. 1A). Subsequently, we performed a comprehensive analysis of the tissue structure and mandibular joint conditions in whole skeletally stained zebrafish to enhance precision in drug injection positioning and angles (Fig. 1B). Upon closure of the mandibular joint, the upper and lower joint surfaces exhibited tight articulation, resulting in a narrow joint space (Fig. 1C). Conversely, upon opening the mandibular joint, the joint space became visible (Fig. 1D). Taking advantage of this distinctive feature of the mandibular joint, we devised a simple and practical injection mold. Zebrafish were positioned in a supine orientation post-anesthetization and immobilized within the mold. By opening the mandibular joint, we could effectively inject drugs into the joint space (Fig. 1E).

Development of a drug jaw joint injection model in zebrafish

To implement our proposed design, we selected a 10 cm dish as the mold container. It was filled it with 30 mL of 1% agarose gel and 3 µl of methylene blue, after which a 2–3 mm wide barrier was inserted into the gel. The mixture was allowed to solidify at room temperature, following which the barrier was carefully removed (Fig. 2A). For drug injection into the joint cavity, a single-channel thin-walled glass capillary (#TW100-4, Word Precision Instruments, America) was selected. Using a horizontal puller (#PN-30, Narishge, Japan), a glass injection needle was crafted with a small opening at the tip, creating using a 15° bevel cutting knife (Fig. 2B). The prepared glass injection needle was attached to the injector, and a stereomicroscope (#SZX2-ILLD, OLYMPUS, JAPAN) served as the injection platform, with an external light source (#LG-PS2-5, OLYMPUS, JAPAN). Following the anesthesia of the zebrafish with 0.2% tricaine, they were positioned in a supine posture in the slot, enabling the mandibular joint to open and rest against the slot's edge (Fig. 2C). The angle of the external light source was adjusted to illuminate the zebrafish mandibular joint clearly under the microscope (Fig. 2D). The needle was carefully inserted into the joint cavity, with a noticeable breakthrough sensation upon penetration (Fig. 2E). A pneumatic picopump (#PV820, WPI, USA) was employed as the drug injector, with the eject pressure set at 20 psi. The single injection volume is approximately 0.03 µL. Upon completing the injection, the needle was gently withdrawn from the joint cavity (Supplementary material 1). Subsequently, the zebrafish were promptly transferred from the injection slot to fresh egg water, and continuous monitoring was maintained until the zebrafish fully recovered before being reintroduced into the breeding system.

Morphological changes were observed in the cartilage of jaw joint after MIA and CTII treatment

We chose the chemical inducers MIA and CTII, commonly utilized in other animal models of osteoarthritis[10,12], for injection into the mandibular joints of zebrafish. To visually observe the morphological changes in the tissue post-injection, we conducted histological staining of the mandibular joints. After 14 days following injection, H&E staining revealed the presence of multinucleated cells (highlighted by yellow arrows), chondrocytes swelling (marked by blue arrows), and fibrosis on the joint surface (indicated by black arrows) in the MIA and CTII groups, indicating notable inflammatory responses and cartilage destruction (Fig. 3A). Statistical analysis revealed differences in the areas of inflammatory infiltration (Fig. 3B-C), cartilage damage (Fig. 3D), and single chondrocyte area (Fig. 3E) between the experimental and control groups. By day 28 post-injection, the experimental group exhibited expanded joint damage, showcasing prominent cartilage defects (indicated by black arrows), chondrocytes hypertrophy (indicated by blue arrows), and apoptosis (indicated by yellow arrows),

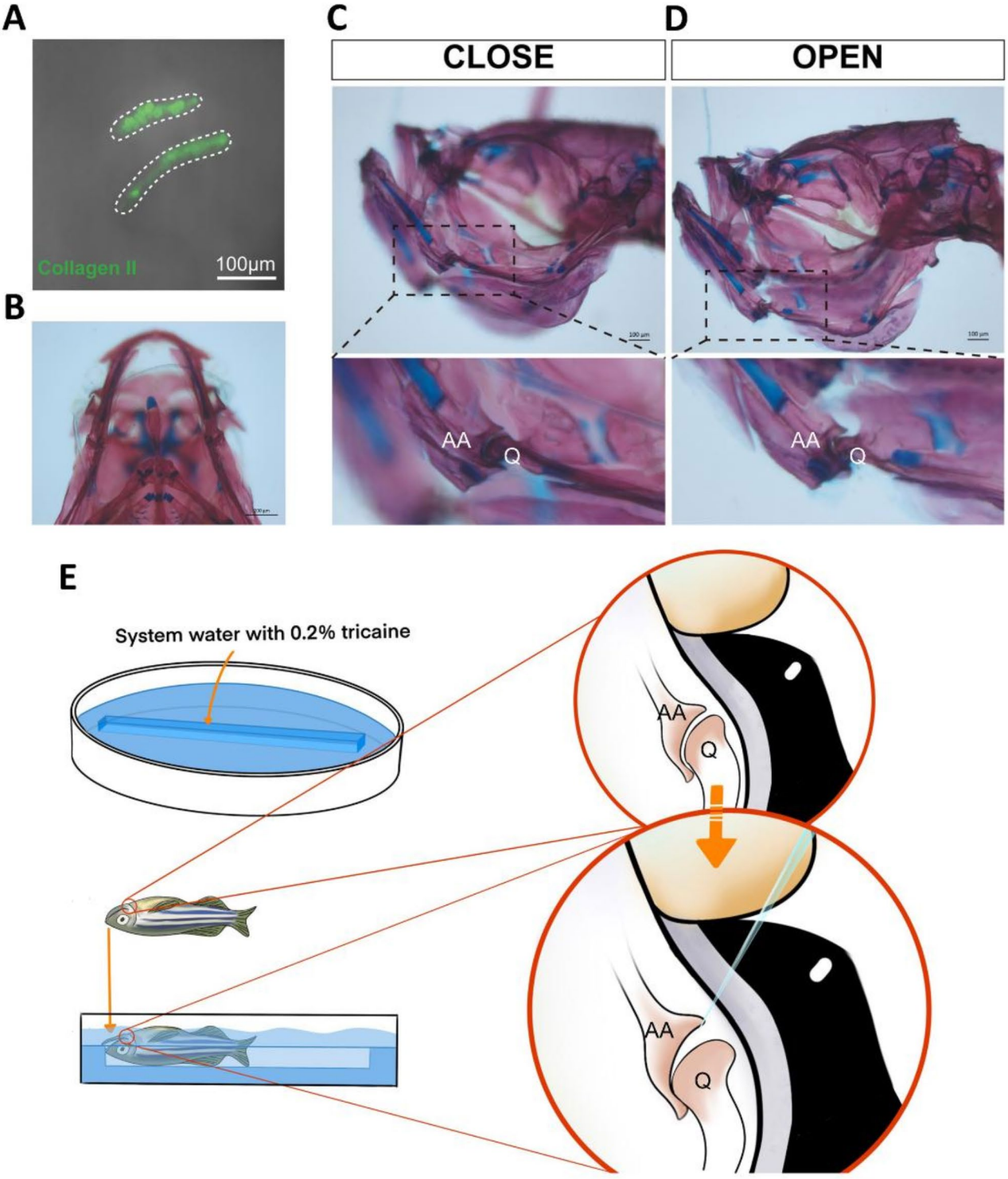

Fig. 1. The zebrafish jaw joint was designated as a modelling joint. (**A**) Col2a1a: EGFP expression was widely observed on the surface cartilage of adult zebrafish jaw joint. (**B**–**D**) Alizarin red-Alcian blue staining of the whole skull of adult zebrafish and two states of the jaw joint were presented, including closed and opened. (**E**) Schematic diagram of zebrafish immobilization, in which zebrafish were immobilized in a supine position in an anesthetic-containing water, with the anterior end of the jaw placed in a groove at the top, and the jaw joint opened.

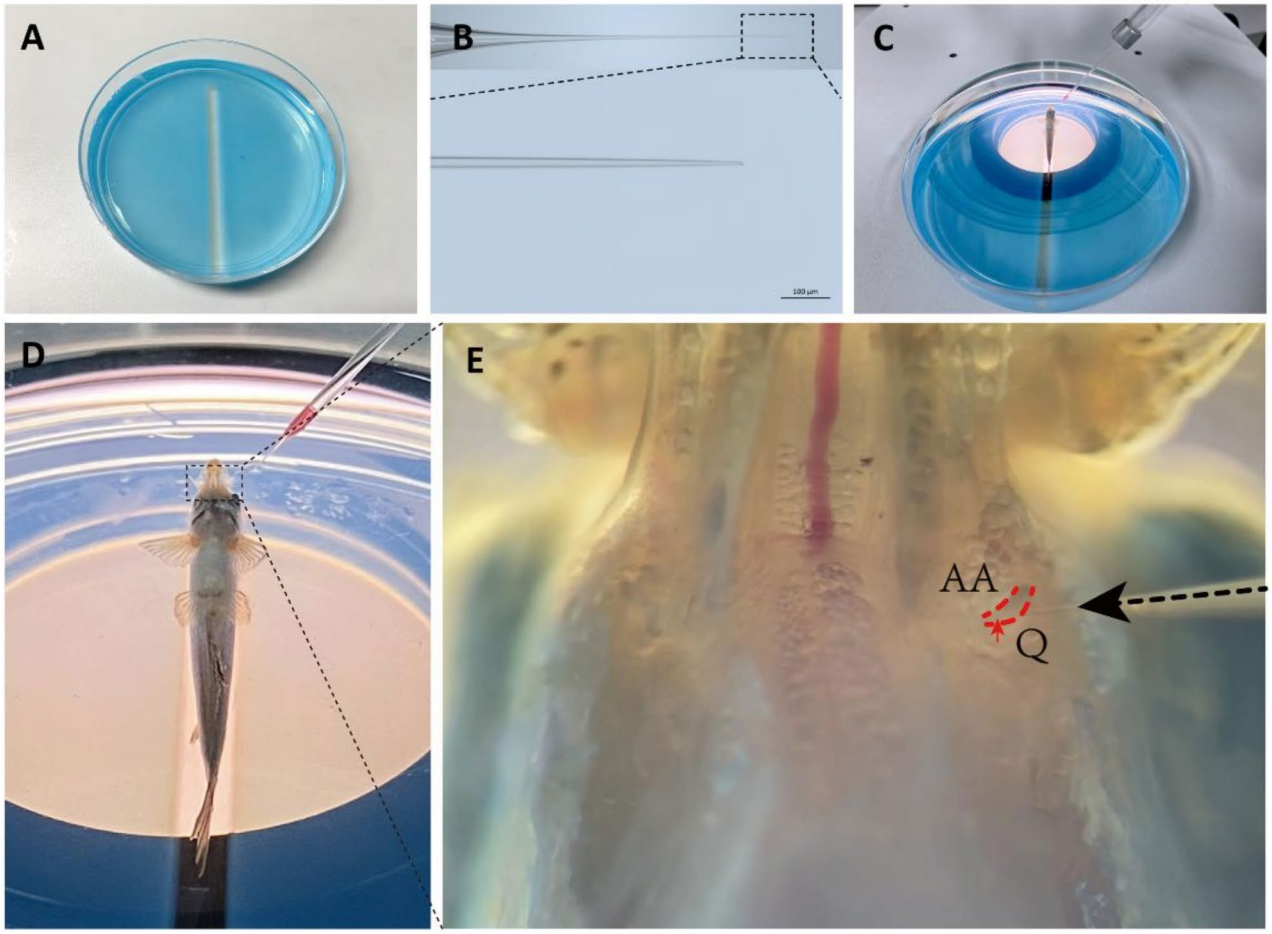

Fig. 2. Figure 2 Development of a drug jaw joint injection model in zebrafish. (**A**) Fabrication of the immobilization mold using agarose gel. (**B**) Preparation of the glass capillary needle using a 15° slanted blade. (**C**) Zebrafish immobilization and angle adjustment. (**D**–**E**) Injection process, including exposing the jaw joint (red dashed lines), needle insertion (black dashed arrow), injection and needle retraction. AA, anguloarticular bone; Q, quadrate bone.

reflecting typical degenerative alterations (Fig. 3F). Further statistical analyses validated these observations (Fig. 3G-J).

OARSI scoring for the mandibular joints of zebrafish

To comprehensively evaluate and quantify osteoarthritis in the mandibular joints of zebrafish, we conducted Safranin O/Fast Green staining at various time points following injection. At 7 dpi (Fig. 4A), both the MIA and CTII groups exhibited incomplete mandibular joint morphology, reduced cartilage matrix, loss of chondrocyte details, and initial subchondral bone involvement. By 14 dpi, the zebrafish mandibular joint cartilage surface displayed irregular features, such as partial disappearance of surface cells, significant wear, hypertrophic chondrocytes, and disorganized arrangement compared to the control group (Fig. 4B). At 28 dpi, additional cartilage wear, erosion of the joint capsule, severe loss of chondrocytes, appearance of vertical clefts, and evident degenerative changes in cartilage were observed (Fig. 4C). Subsequently, we evaluated the extent of damage in the zebrafish mandibular joint surface cartilage using the modified OARSI scoring system. By 7 dpi, the 3% MIA group had already shown scores exceeding 6 (indicating mild damage) for 3 out of 12 mandibular joint surfaces. In contrast, the 1% CTII group, while not surpassing scores of 6, had 7 out of 16 joints with scores reaching 6. This was in contrast to the control group, where scores generally ranged within 0–2 (Fig. 4D-E). By 14 dpi, over half of the joints in both drug-treated groups had scores exceeding 6 (Fig. 4F-G). By 28 dpi, nearly all joint surfaces exhibited varying degrees of damage (Fig. 4H-I). At this time, the highest average OARSI scores for the 3% MIA group was 18.5, while the 1% CTII group reached 14.5. (Fig. 4J). Notably, despite variations in the timing of mandibular joint surface cartilage degeneration post-injection and the progression over time, our results supported the conclusion that OA was effectively induced in the zebrafish mandibular joint following MIA and CTII injections.

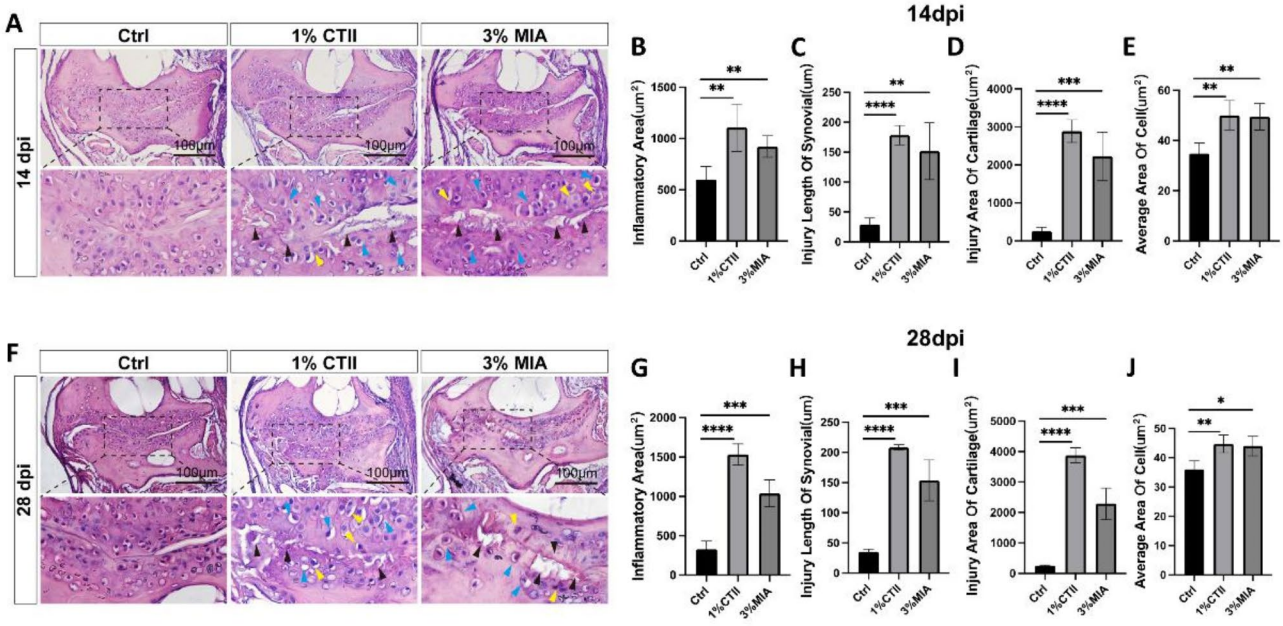

Fig. 3. Morphological changes were observed in the cartilage of the jaw joint after administration of MIA and CTII. (**A**) HE staining of the jaw joint in the control group and drug-injected groups at 14 dpi. (**B**–**E**) Statistical analysis of inflammatory area, injury length of synovial, injury area of cartilage, and average area of cell between control and experimentao groups at 14 dpi. (**F**) HE staining of the jaw joint in the control group and drug-injected groups at 28 dpi. (**G**–**J**) Statistical analysis of inflammatory area, injury length of synovial, injury area of cartilage, and average area of cell between control and experimentao groups at 28 dpi. *P < 0.05, **P < 0.01, ***P < 0.001, ****P < 0.0001. All data were from n=5 zebrafish in each group.

Aggrecan, Adamts5 and MMP13 expression in the zebrafish OA model

After successfully inducing OA in the zebrafish mandibular joint, our study delved into investigating changes in the expression of the synthesis and degradation markers Aggrecan, Adamts5 and MMP13 in OA chondrocytes at various time points through immunohistochemistry. These markers have long been associated with OA in existing literature[28–30]. At 7 dpi, notable differences in Aggrecan expression in the MIA and CTII groups compared to the control group were apparent (Fig. 5A). The robust expression of Aggrecan in the extracellular matrix crucial for cartilage formation markedly decreased in the MIA and CTII groups (Fig. 5B), indicating an early-stage loss of extracellular matrix in the development of OA in the zebrafish mandibular joint. Conversely, the positive expression of Adamts5 and MMP13 began to increase in all groups, highlighting their essential role in degrading joint cartilage tissue (Fig. 5C-D). These observations confirmed the presence of OA in the zebrafish mandibular joint. By 14 dpi, the decline in Aggrecan expression persisted in the MIA and CTII groups (Fig. 5E-F), while Adamts5 and MMP13 exhibited widespread, robust positive expression on the mandibular joint surface (Fig. 5G-H). At this stage, noticeable chondrocyte hypertrophy and irregular chondrocytes arrangement near the injury site indicated the typical progression of OA with reduced cartilage matrix and concurrent abnormal changes in chondrocytes. Continued monitoring at 28 dpi revealed immunohistochemical outcomes similar to those at 14 dpi (Fig. 5I-L), aligning with our initial hypotheses. Despite this, the positive expression patterns of Aggrecan, Adamts5 and MMP13 mirrored those at 14 dpi. Nevertheless, our experimental results unequivocally confirmed the induction and progression of OA in the zebrafish mandibular joint post-drug injection.

The expression of collagen II was decreased in living zebrafish following the modeling process

Having successfully established the OA model in the zebrafish mandibular joint, we proceeded to validate the model in vivo using the pre-established *Tg (col2a1a: EGFP)* cq77 zebrafish line. As anticipated, live confocal imaging results in vivo unveiled a significant reduction in Collagen II expression in the mandibular joint surface cartilage (Fig. 6).

Discussion

In this study, zebrafish were chosen as the model organism for OA due to several advantageous characteristics. Zebrafish are small in size, exhibit rapid development, boast large population numbers, and are cost-effective to breed, providing key advantages for OA research. Notably, zebrafish share a substantial genetic and molecular resemblance to humans[31], making them a promising model for unraveling the underlying pathogenic mechanisms of OA and assessing potential therapeutic targets. The zebrafish mandibular joint, being the largest joint in the organism with a hinged structure, allows for easy opening and closing of the joint space, facilitating experimental procedures and observation. Classified as a synovial joint, it shares similarities with human synovial

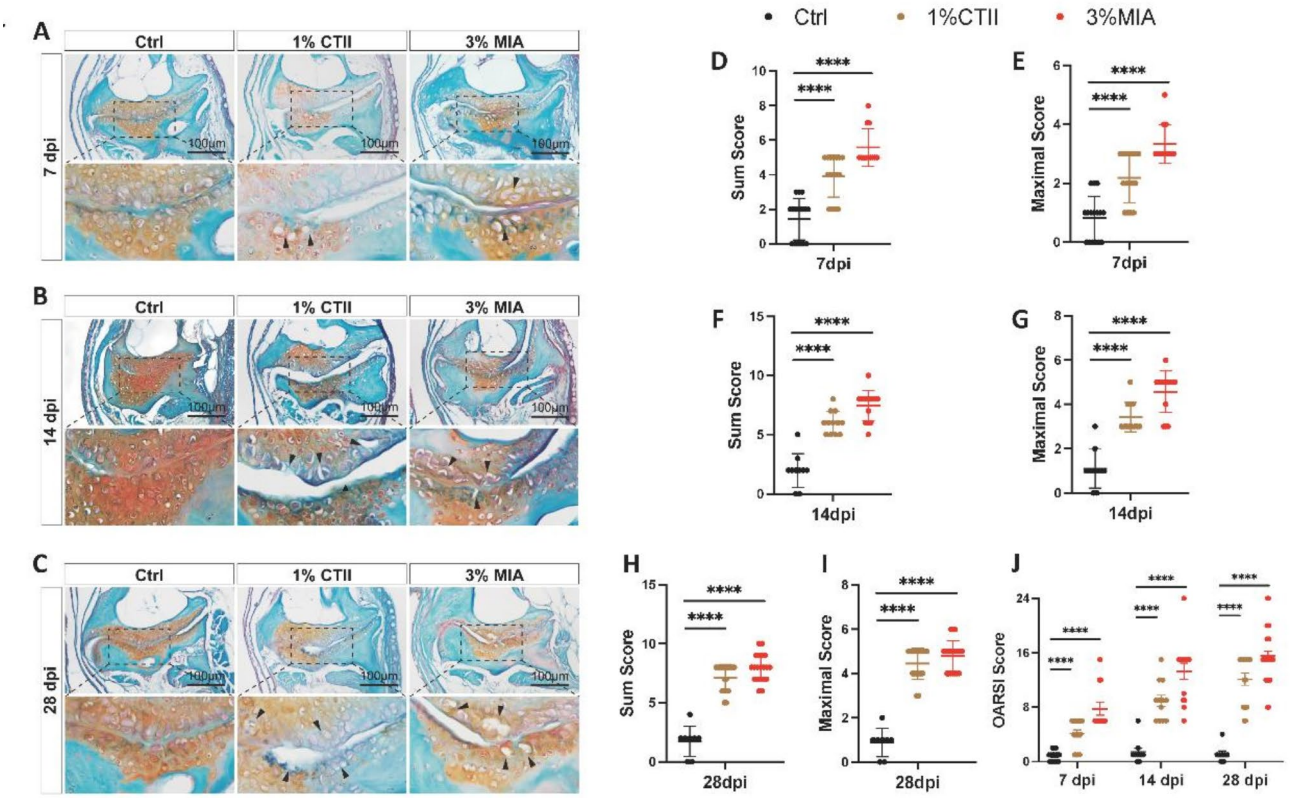

Fig. 4. OARSI scoring for the mandibular joints of zebrafish. (**A**–**C**) Safranin O-Fast Green staining of the jaw joint in the control group and drug-injected groups at 7, 14 and 28 dpi. (**D**–**E**) Quantification of degenerative changes in joint cartilage at 7 dpi using the modified Zebrafish OARSI scoring method. (**F**–**G**) Quantification of degenerative changes in joint cartilage at 14 dpi. (**H**–**I**) Quantification of degenerative changes in joint cartilage at 28 dpi. (**J**) Statistical analysis of OARSI scores among 7, 14 and 28 dpi. ****P < 0.0001. All data were from n=5 zebrafish in each group.

joints. Additionally, zebrafish offer rapid gene-editing capabilities, a significant advantage for in vivo dynamic imaging of the joint. Consequently, the zebrafish OA model fulfills the criteria for an economically feasible and genetically manipulable model. Existing zebrafish models primarily involve surgical interventions to sever ligaments[22] or utilize gene editing to induce joint damage[23]. These current models mainly concentrate on the study of development and regeneration as well as genetic diseases. Our model induces cartilage damage through chemical means to simulate the degenerative progression of OA, thus allowing for a more accurate description of the disease's pathology and progression. Given the transparency of zebrafish, researchers are able to observe changes in cartilage and joint structures in real time, providing insights into the dynamic processes associated with OA. By leveraging the unique attributes of zebrafish, researchers can delve deep into the molecular and cellular processes involved in OA progression, identifying novel therapeutic targets for personalized medicine. However, the zebrafish OA model has certain limitations. The mandibular joint of zebrafish is non-weight-bearing, which leads to a lack of biomechanical relationships akin to those observed in OA. Moreover, zebrafish are exposed to distinct environmental conditions compared to humans, resulting in significant physiological and metabolic differences that diminish the accuracy of OA modeling when compared to other animal models. Additionally, the small size of the zebrafish mandibular joint poses challenges for various laboratory assessments commonly used to evaluate OA, such as X-rays and micro-computed tomography (microCT), making their application more complex than in larger animal models.

Our study introduced a specially designed mold to effectively immobilize zebrafish and exposes the jaw joints, simplifying the process of drug injection into the joint cavity. Unlike conventional animal models, our method offers convenience, immediacy and precision in drug injection. In traditional models, fur removal is typically required before injection, leading to extended procedural time, increased risk of skin damage and potential infection. Moreover, in comparison to human joints, rodent joints, such as those in rats, are considerably smaller in size. This diminutive size poses challenges when administering drugs, necessitating a high level of skill and precision from operators to ensure accurate localization and dosing, potentially introducing experimental bias. Zebrafish, on the other hand, do not require fur removal and have shallow jaw joint locations that allow for direct visualization under a microscope. By utilizing a microinjection apparatus, precise control over dosage administration is achieved, optimizing the experimental workflow, reducing reliance on operator expertise, enhancing success rates, and minimizing experimental inaccuracies.

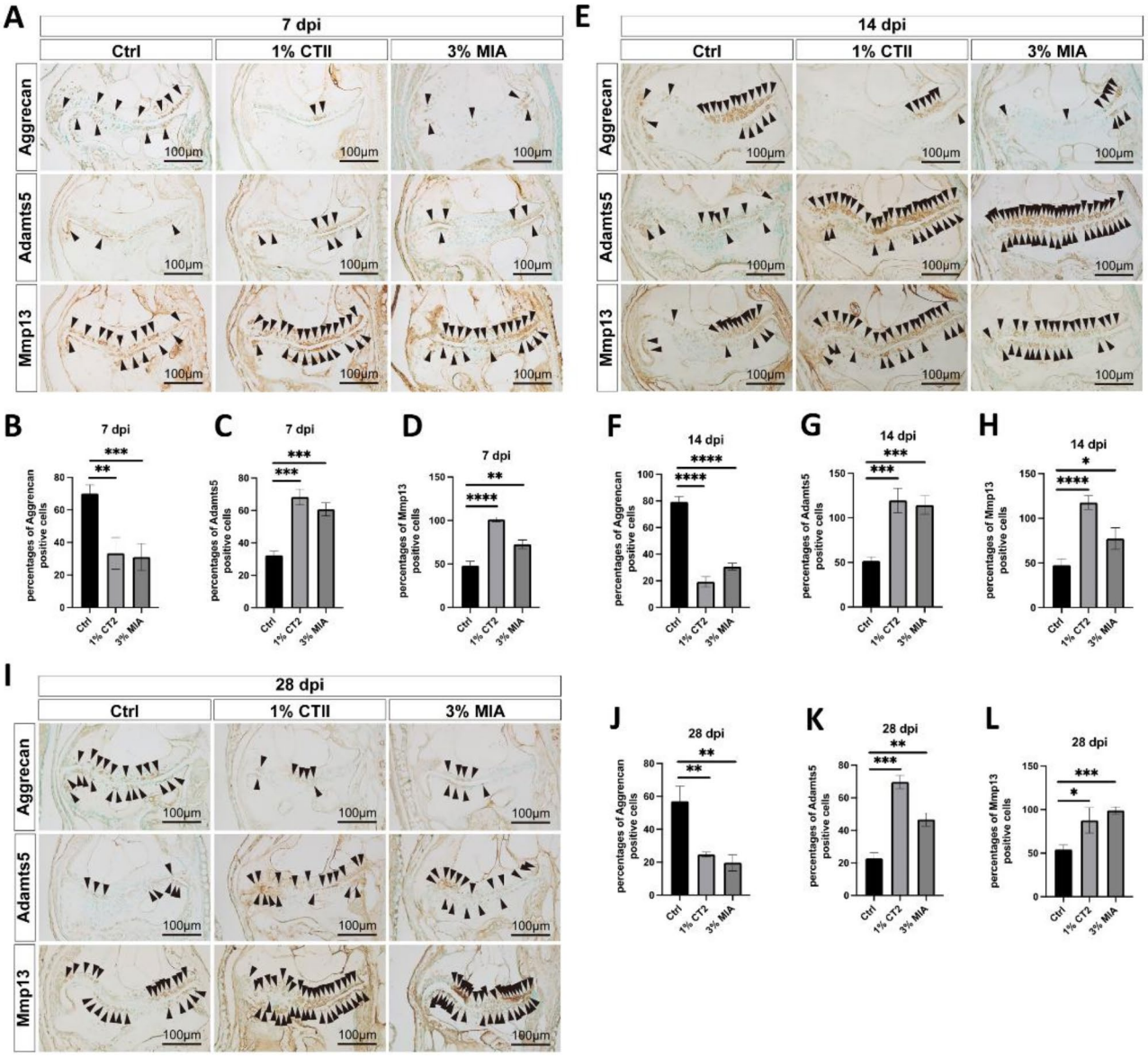

Fig. 5. Aggrecan, Adamts5 and MMP13 expression in zebrafish OA model. (**A**–**D**) Immunohistochemical staining and relative quantitative analysis of Aggrecan, Adamts5 and MMP13 at 7 dpi. (**E**–**H**) Immunohistochemical staining and relative quantitative analysis of Aggrecan, Adamts5 and MMP13 at 14 dpi. (**I**–**L**) Immunohistochemical staining and relative quantitative analysis of Aggrecan, Adamts5 and MMP13 at 28 dpi. *P < 0.05, **P < 0.01, ***P < 0.001, ****P < 0.0001. All data were from n=5 zebrafish in each group..

In our study, we identified hypertrophic chondrocytes within the control group. To confirm this finding, we established a blank control group comprising normally developed zebrafish. The presence of hypertrophic chondrocytes in this control group suggested that a degree of spontaneous hypertrophy can occur as part of the zebrafish's natural physiological processes, even without induced osteoarthritis. Our analysis indicates that various factors, including age, may contribute to this phenomenon. In an effort to closely mimic the onset of OA, we selected experimental animals that were one year old, despite zebrafish typically reaching maturity at three months. Furthermore, we noted that areas featuring hypertrophic chondrocytes were predominantly concentrated at the injection sites, where the injection needle potentially caused direct damage to the adjacent cartilage and subchondral bone, introducing associated experimental biases. A comprehensive examination across multiple time points highlighted distinct differences between the control and experimental groups. In the experimental group, hypertrophic chondrocytes were more pronounced and widespread, showcasing significant pathological alterations. Our results suggest that while some cartilage may exhibit mild hypertrophic changes, these changes are markedly intensified in the specific compartmentalized responses induced by MIA and CTII injections.

While specific histological markers for zebrafish OA specimens are currently lacking, histopathology remains the gold standard for evaluating animal models of OA[32,33]. In our study, we employed established histological

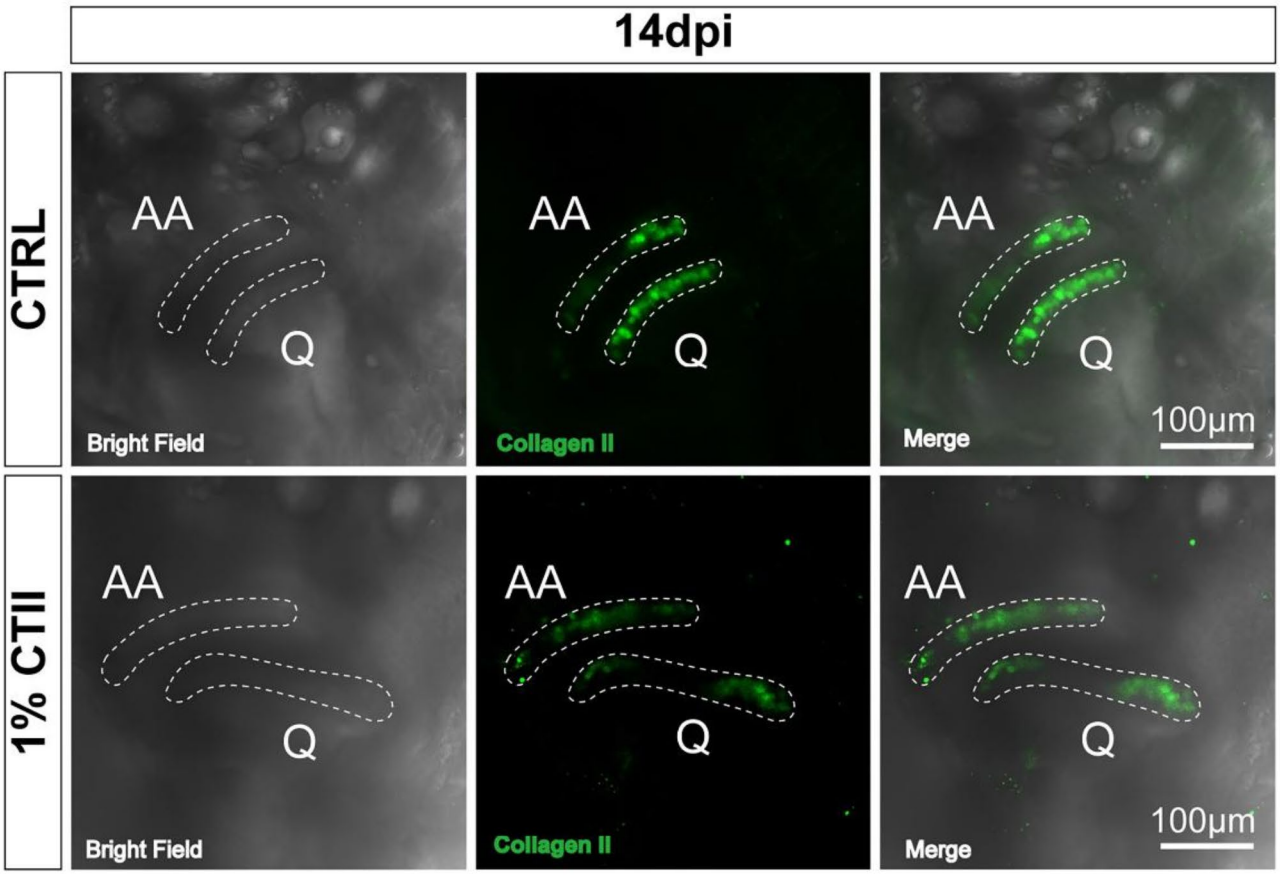

Fig. 6. The expression of Collagen II in living zebrafish following the modeling process. At 14 dpi, there was a significant reduction of Collagen II expression on the surface of the jaw joint cartilage, indicating significant cartilage destruction.

analysis techniques, such as H&E staining of jaw joint sections to assess overall structures and cellular characteristics. Subsequent evaluation of glycosaminoglycan (GAG) distribution was conducted through Safranin O/Fast Green staining. Safranin O, a basic dye, binds strongly to proteoglycans in cartilage, resulting in an orange color. Damaged cartilage releases glycoproteins, leading to reduced or absent Safranin O staining and an uneven distribution of matrix components. Quantitative assesment of the stained cartilage matrix was performed using image analysis software. Additionally, we utilized the OARSI scoring system to analyze jaw joint specimens, revealing notable distinctions between the drug-injected group and the control group. Furthermore, immunohistochemical staining was employed to detect the expression levels of Aggrecan, Adamts5 and MMP13 in jaw joint cartilage to evaluate pathological changes. Aggrecan, a proteoglycan composed of GAG and core protein, plays a crucial role as a structural component of cartilage[34]. Adamts5, a disintegrin and metalloproteinase with thrombospondin motifs, primarily degrades aggrecan in articular cartilage matrix[29]. While MMP13, a matrix metalloproteinase, is capable of degrading type II collagen in the extracellular matrix of cartilage[35]. Our experimental results revealed a significant decrease in Aggrecan expression and an increase in the levels of Adamts5 and MMP13 in the drug-injected group compared to the control group. Finally, utilizing the heritable marking trait of zebrafish, live imaging technology was employed to visualize the entire jaw joint, demonstrating pronounced signal loss in the jaw joint cartilage following drug injection. This discovery reaffirmed the effective induction of OA in the zebrafish mandibular joint and provided vital insights into the in vivo manifestation of the disease within this model. In summary, these experimental findings collectively strengthen the evidence of varying degrees of OA occurrence in the zebrafish jaw joint.

OA typically manifests with clinical symptoms primarily characterized by pain, making pain relief the most predominant therapeutic focus[36]. Utilizing a behavioral tracking system to capture data such as the frequency and duration of fast and slow movements, distance, speed, and average velocity enables effective pain assessment in the zebrafish model[37]. Moreover, integrating the zebrafish model into the drug discovery process confers several advantages over traditional methods[38,39]. These benefits encompass early identification of in vivo safety concerns linked to candidate compounds, timely recognition of potential efficacy issues, and the capacity to assess absorption and metabolic challenges. Additionally, the zebrafish model yields comprehensive efficacy-based screening outcomes that surpass what can be achieved through in vitro approaches, ultimately leading to reduced development timelines, costs, and enhanced success rates. Furthermore, the zebrafish model can

replicate the degenerative alterations associated with OA[40], facilitating the exploration of the ossification processes of articular cartilage[41] and delving into the underlying mechanisms of the disease[42,43].

Furthermore, considering the limited regenerative capacity of cartilage in most mammals, intra-articular drug injections that cause cartilage damage can lead to irreversible joint deterioration in OA. In contrast, zebrafish, in comparison to conventional animal models like mice, demonstrate a superior ability for cartilage regeneration. This model allows for the specific investigation of the body's response to cartilage damage, including regeneration mechanisms and factors that promote or inhibit healing. Recent findings by Dora Sapède et al.[44] have revealed that zebrafish larvae can regenerate their cartilage post-injury through the Nrg1/ErbB pathway. This discovery not only opens new avenues for researchers but also holds significant implications for understanding cartilage regeneration mechanisms and enhancing the regenerative potential of mammalian cartilage.

Looking ahead, investigations centered on the zebrafish OA model are poised to delve deeper into the genetic and environmental factors influencing OA susceptibility and progression. Moreover, the model's effectiveness in drug screening and live imaging holds promise for advancing our understanding of OA pathogenesis and expediting the discovery of effective treatments. Ultimately, the OA model is set to revolutionize OA research and make substantial contributions to the progress of precision medicine in managing this debilitating joint ailment.

Conclusion

In our study, we chose zebrafish as the experimental model organism. Capitalizing on the distinctive anatomical features of the zebrafish mandibular joint, we developed a straightforward fixation device and effectively administered drugs into the joint cavity using a microinjector. Through the injection of MIA and CTII into the joint cavity, we were able to induce the pathological changes characteristic of OA in the zebrafish mandibular joint. Our research aims to complement and enhance existing animal models by leveraging the unique advantages of the zebrafish species. In the future, it will focus on the development of new drugs and the study of cartilage regeneration, providing a theoretical foundation and new therapeutic perspectives for the prevention and treatment of OA.

Data availability

The authors confirm that the data supporting the findings of this study are available from the corresponding author on reasonable request.

Received: 25 August 2024; Accepted: 24 January 2025
Published online: 31 January 2025

References

1. Martel-Pelletier, J. et al. Osteoarthritis. *Nat. Rev. Dis. Primers*. **2**, 16072. https://doi.org/10.1038/nrdp.2016.72 (2016).
2. Sanchez-Lopez, E., Coras, R., Torres, A., Lane, N. E. & Guma, M. Synovial inflammation in osteoarthritis progression. *Nat. Rev. Rheumatol.* **18**, 258–275. https://doi.org/10.1038/s41584-022-00749-9 (2022).
3. Motta, F., Barone, E., Sica, A. & Selmi, C. Inflammaging and osteoarthritis. *Clin. Rev. Allergy Immunol.* **64**, 222–238. https://doi.org/10.1007/s12016-022-08941-1 (2023).
4. Glyn-Jones, S. et al. *Osteoarthr. Lancet* **386**, 376–387 https://doi.org/10.1016/s0140-6736(14)60802-3 (2015).
5. Katz, J. N., Arant, K. R. & Loeser, R. F. Diagnosis and treatment of hip and knee osteoarthritis: a review. *Jama* **325**, 568–578. https://doi.org/10.1001/jama.2020.22171 (2021).
6. Yue, L., Berman, J. & What *Is Osteoarthritis? Jama* **327**, 1300 https://doi.org/10.1001/jama.2022.1980 (2022).
7. van der Kraan, P. M., Vitters, E. L., van Beuningen, H. M., van de Putte, L. B. & van den Berg, W. B. Degenerative knee joint lesions in mice after a single intra-articular collagenase injection. A new model of osteoarthritis. *J. Exp. Pathol. (Oxford)*. **71**, 19–31 (1990).
8. Kamekura, S. et al. Osteoarthritis development in novel experimental mouse models induced by knee joint instability. *Osteoarthr. Cartil.* **13**, 632–641. https://doi.org/10.1016/j.joca.2005.03.004 (2005).
9. Staines, K. A., Poulet, B., Wentworth, D. N. & Pitsillides, A. A. The STR/ort mouse model of spontaneous osteoarthritis - an update. *Osteoarthr. Cartil.* **25**, 802–808. https://doi.org/10.1016/j.joca.2016.12.014 (2017).
10. Guzman, R. E., Evans, M. G., Bove, S., Morenko, B. & Kilgore, K. Mono-iodoacetate-induced histologic changes in subchondral bone and articular cartilage of rat femorotibial joints: an animal model of osteoarthritis. *Toxicol. Pathol.* **31**, 619–624. https://doi.org/10.1080/01926230390241800 (2003).
11. Høegh-Andersen, P. et al. Ovariectomized rats as a model of postmenopausal osteoarthritis: validation and application. *Arthritis Res. Ther.* **6**, R169–180. https://doi.org/10.1186/ar1152 (2004).
12. Kikuchi, T., Sakuta, T. & Yamaguchi, T. Intra-articular injection of collagenase induces experimental osteoarthritis in mature rabbits. *Osteoarthr. Cartil.* **6**, 177–186. https://doi.org/10.1053/joca.1998.0110 (1998).
13. Shen, S. et al. CircSERPINE2 protects against osteoarthritis by targeting miR-1271 and ETS-related gene. *Ann. Rheum. Dis.* **78**, 826–836. https://doi.org/10.1136/annrheumdis-2018-214786 (2019).
14. Kim, J. E., Song, D. H., Kim, S. H., Jung, Y. & Kim, S. J. Development and characterization of various osteoarthritis models for tissue engineering. *PLoS One*. **13**, e0194288. https://doi.org/10.1371/journal.pone.0194288 (2018).
15. Endisha, H. et al. MicroRNA-34a-5p promotes Joint Destruction during Osteoarthritis. *Arthritis Rheumatol.* **73**, 426–439. https://doi.org/10.1002/art.41552 (2021).
16. Little, C. B. & Zaki, S. What constitutes an animal model of osteoarthritis--the need for consensus? *Osteoarthr. Cartil.* **20**, 261–267. https://doi.org/10.1016/j.joca.2012.01.017 (2012).
17. Zaki, S., Blaker, C. L. & Little, C. B. OA foundations - experimental models of osteoarthritis. *Osteoarthr. Cartil.* **30**, 357–380. https://doi.org/10.1016/j.joca.2021.03.024 (2022).
18. Patton, E. E., Zon, L. I. & Langenau, D. M. Zebrafish disease models in drug discovery: from preclinical modelling to clinical trials. *Nat. Rev. Drug Discov*. **20**, 611–628. https://doi.org/10.1038/s41573-021-00210-8 (2021).
19. Busse, B., Galloway, J. L., Gray, R. S., Harris, M. P. & Kwon, R. Y. Zebrafish: an emerging model for Orthopedic Research. *J. Orthop. Res.* **38**, 925–936. https://doi.org/10.1002/jor.24539 (2020).
20. Mitchell, R. E. et al. New tools for studying osteoarthritis genetics in zebrafish. *Osteoarthr. Cartil.* **21**, 269–278. https://doi.org/10.1016/j.joca.2012.11.004 (2013).

21. Zappia, J. et al. Osteomodulin downregulation is associated with osteoarthritis development. *Bone Res.* **11**, 49. https://doi.org/10.1038/s41413-023-00286-5 (2023).
22. Smeeton, J. et al. Regeneration of Jaw Joint cartilage in adult zebrafish. *Front. Cell. Dev. Biol.* **9**, 777787. https://doi.org/10.3389/fcell.2021.777787 (2021).
23. Askary, A. et al. Ancient origin of lubricated joints in bony vertebrates. *Elife* **5** https://doi.org/10.7554/eLife.16415 (2016).
24. Lawrence, E. A. et al. The mechanical impact of col11a2 loss on joints; col11a2 mutant zebrafish show changes to joint development and function, which leads to early-onset osteoarthritis. *Philos. Trans. R Soc. Lond. B Biol. Sci.* **373** https://doi.org/10.1098/rstb.2017.0335 (2018).
25. Choi, J. H. et al. Effects of SKI 306X, a new herbal agent, on proteoglycan degradation in cartilage explant culture and collagenase-induced rabbit osteoarthritis model. *Osteoarthr. Cartil.* **10**, 471–478. https://doi.org/10.1053/joca.2002.0526 (2002).
26. Sprague, J. et al. The Zebrafish Information Network: the zebrafish model organism database provides expanded support for genotypes and phenotypes. *Nucleic Acids Res.* **36**, D768–772. https://doi.org/10.1093/nar/gkm956 (2008).
27. Kim, S. W. et al. Current status of the zebrafish euthanasia and Humane Endpoint in the Republic of Korea and Guideline Suggestion from Nationwide Expert Elicitation: a model for other Countries. *Zebrafish* **21**, 53–66. https://doi.org/10.1089/zeb.2023.0086 (2024).
28. Wei, Y. et al. Targeting cartilage EGFR pathway for osteoarthritis treatment. *Sci. Transl Med.* **13** https://doi.org/10.1126/scitranslmed.abb3946 (2021).
29. Jiang, L. et al. ADAMTS5 in Osteoarthritis: Biological functions, Regulatory Network, and potential targeting therapies. *Front. Mol. Biosci.* **8**, 703110. https://doi.org/10.3389/fmolb.2021.703110 (2021).
30. Hu, Q. & Ecker, M. Overview of MMP-13 as a Promising Target for the treatment of Osteoarthritis. *Int. J. Mol. Sci.* **22** https://doi.org/10.3390/ijms22041742 (2021).
31. Howe, K. et al. The zebrafish reference genome sequence and its relationship to the human genome. *Nature* **496**, 498–503. https://doi.org/10.1038/nature12111 (2013).
32. Pauli, C. et al. Comparison of cartilage histopathology assessment systems on human knee joints at all stages of osteoarthritis development. *Osteoarthr. Cartil.* **20**, 476–485. https://doi.org/10.1016/j.joca.2011.12.018 (2012).
33. Appleton, C. T., McErlain, D. D., Henry, J. L., Holdsworth, D. W. & Beier, F. Molecular and histological analysis of a new rat model of experimental knee osteoarthritis. *Ann. N Y Acad. Sci.* **1117**, 165–174. https://doi.org/10.1196/annals.1402.022 (2007).
34. Kiani, C., Chen, L., Wu, Y. J., Yee, A. J. & Yang, B. B. Structure and function of aggrecan. *Cell. Res.* **12**, 19–32. https://doi.org/10.1038/sj.cr.7290106 (2002).
35. Wang, X., Khalil, R. A., Matrix & Metalloproteinases Vascular remodeling, and Vascular Disease. *Adv. Pharmacol.* **81**, 241–330. https://doi.org/10.1016/bs.apha.2017.08.002 (2018).
36. Yu, H., Huang, T., Lu, W. W., Tong, L. & Chen, D. Osteoarthritis Pain. *Int. J. Mol. Sci.* **23** https://doi.org/10.3390/ijms23094642 (2022).
37. Ohnesorge, N., Heinl, C. & Lewejohann, L. Current methods to Investigate Nociception and Pain in zebrafish. *Front. Neurosci.* **15**, 632634. https://doi.org/10.3389/fnins.2021.632634 (2021).
38. Seda, M. et al. An FDA-Approved drug screen for compounds Influencing Craniofacial skeletal development and craniosynostosis. *Mol. Syndromol.* **10**, 98–114. https://doi.org/10.1159/000491567 (2019).
39. MacRae, C. A. & Peterson, R. T. Zebrafish as tools for drug discovery. *Nat. Rev. Drug Discov.* **14**, 721–731. https://doi.org/10.1038/nrd4627 (2015).
40. Hayes, A. J. et al. Spinal deformity in aged zebrafish is accompanied by degenerative changes to their vertebrae that resemble osteoarthritis. *PLoS One.* **8**, e75787. https://doi.org/10.1371/journal.pone.0075787 (2013).
41. Eames, B. F. et al. Mutations in fam20b and xylt1 reveal that cartilage matrix controls timing of endochondral ossification by inhibiting chondrocyte maturation. *PLoS Genet.* **7**, e1002246. https://doi.org/10.1371/journal.pgen.1002246 (2011).
42. Lawrence, E. A., Hammond, C. L. & Blain, E. J. Potential of zebrafish as a model to characterise MicroRNA profiles in mechanically mediated joint degeneration. *Histochem. Cell. Biol.* **154**, 521–531. https://doi.org/10.1007/s00418-020-01918-1 (2020).
43. Raman, R. et al. A zebrafish mutant in the Extracellular matrix protein gene efemp1 as a model for spinal osteoarthritis. *Anim. (Basel).* 14. https://doi.org/10.3390/ani14010074 (2023).
44. Sapède, D. et al. Cartilage regeneration in zebrafish depends on Nrg1/ErbB signaling pathway. *Front. Cell. Dev. Biol.* **11**, 1123299. https://doi.org/10.3389/fcell.2023.1123299 (2023).

Acknowledgements
Not applicable.

Author contributions
GX, XS and JQ designed this study. GX, JQ, RZ and JH performed the experiments. YM and WL gave help in the production of schematic diagram. GX, HY and QS analyzed the data and wrote the manuscript. MN and XS revised the paper and gave final approval. All authors reviewed the manuscript.

Funding
This work is supported by research funding from the National Natural Science Foundation of China (No. 82372397, 82002307), Natural Science Foundation of Chongqing (cstc2022ycjh-bgzxm0052), Chongqing Talent Project (CQYC202105025), Chongqing Postdoctoral Program for Innovative Talents (CQBX202209) and Kuanren Talents Program of the second affiliated hospital of Chongqing Medical University.

Declarations

Competing interests
The authors declare no competing interests.

Ethics approval and consent to participate
This study was approved by Institutional Animal Care and Use Committee of the Research Institute of Surgery, Daping Hospital IACUC protocol SYXK- (Army) 2022-0003 and performed in strict with the institutional guidelines for care and use of laboratory animals.

Additional information

Supplementary Information The online version contains supplementary material available at https://doi.org/10.1038/s41598-025-88125-x.

Correspondence and requests for materials should be addressed to X.S. or M.N.

Reprints and permissions information is available at www.nature.com/reprints.

Publisher's note Springer Nature remains neutral with regard to jurisdictional claims in published maps and institutional affiliations.